Low temperature magnetic properties and spin dynamics in single crystals of Cr_8Zn antiferromagnetic molecular rings

Fatemeh Adelnia,[1,2] Alessandro Chiesa,[3] Sara Bordignon,[3] Stefano Carretta,[3] Alberto Ghirri,[4] Andrea Candini,[4] Christian Cervetti,[5] Marco Evangelisti,[4,5,6] Marco Affronte,[4,5] Ilya Sheikin,[7] Richard Winpenny,[8] Grigore Timco,[8] Ferdinando Borsa,[2] and Alessandro Lascialfari[1,2,3]

[1]*Dipartimento di Fisica, Università degli Studi di Milano and INSTM, I-20133 Milano, Italy*
[2]*Dipartimento di Fisica, Università degli Studi di Pavia and INSTM, I-27100 Pavia, Italy*
[3]*Dipartimento di Fisica e Scienze della Terra, Università degli Studi di Parma, I-43124 Parma, Italy*
[4]*CNR Institute Nanosciences S3, I- 41125 Modena, Italy*
[5]*Dipartimento di Scienze Fisiche, Informatiche, Matematiche, Università di Modena e Reggio Emilia, I-41125 Modena, Italy*
[6]*Instituto de Ciencia de Materiales de Aragón and Departamento de Física de la Materia Condensada, CSIC-Universidad de Zaragoza, 50009 Zaragoza, Spain*
[7]*Grenoble High Magnetic Field Laboratory, CNRS-LNCMI, 25, B.P. 166, 38042 Grenoble Cedex 9, France*
[8]*The Lewis Magnetism Laboratory, The University of Manchester, M13 9PL Manchester, United Kingdom*

(Received 11 October 2015; accepted 4 December 2015; published online 31 December 2015)

A detailed experimental investigation of the effects giving rise to the magnetic energy level structure in the vicinity of the level crossing (LC) at low temperature is reported for the open antiferromagnetic molecular ring Cr_8Zn. The study is conducted by means of thermodynamic techniques (torque magnetometry, magnetization and specific heat measurements) and microscopic techniques (nuclear magnetic resonance line width, nuclear spin lattice, and spin-spin relaxation measurements). The experimental results are shown to be in excellent agreement with theoretical calculations based on a minimal spin model Hamiltonian, which includes a Dzyaloshinskii-Moriya interaction. The first ground state level crossing at $\mu_0 H_{c1} = 2.15$ T is found to be an almost true LC while the second LC at $\mu_0 H_{c2} = 6.95$ T has an anti-crossing gap of $\Delta_{12} = 0.19$ K. In addition, both NMR and specific heat measurements show the presence of a level anti-crossing between excited states at $\mu_0 H = 4.5$ T as predicted by the theory. In all cases, the fit of the experimental data is improved by introducing a distribution of the isotropic exchange couplings (J), i.e., using a *J strain* model. The peaks at the first and second LCs in the nuclear spin-lattice relaxation rate are dominated by inelastic scattering and a value of $\Gamma \sim 10^{10}$ rad/s is inferred for the life time broadening of the excited state of the open ring, due to spin phonon interaction. A loss of NMR signal (wipe-out effect) is observed for the first time at LC and is explained by the enhancement of the spin-spin relaxation rate due to the inelastic scattering. [http://dx.doi.org/10.1063/1.4938086]

I. INTRODUCTION

During the last decade, physicists have paid considerable attention to Molecular Nano Magnets (MNMs) as model systems to study fundamental quantum and magnetic properties.[1,2] In many MNMs, the intermolecular magnetic interactions are negligible as compared to the intra-molecular exchange interactions, thus the bulk magnetic properties reflect the microscopic features of individual molecular units. The discovery of quantum phenomena such as the macroscopic quantum tunneling[3,4] of the magnetization and the possibility of applications in magnetic storage and quantum computing,[5,6] has further increased the motivation to study MNMs. Antiferromagnetic Molecular (AFM) rings are an interesting subgroup of MNMs, which are formed by a finite number of transition-metal ions arranged in a cyclic structure. Due to the finite-size effect, a discrete energy spectrum is present in all AFM rings at low temperature with a ground state which can be a singlet with total spin S = 0 or a magnetic ground state depending on the spin topology of the ring. An external magnetic field lifts the degeneracy of M_s, the projection of the total spin (S) of the ring along the quantization axis, inducing Level Crossings (LCs) between the ground state and the excited states. The study of the LCs in AFM rings is a good direct experimental probe of the energy levels structure to be compared with theoretical results[7–9] and it allows the investigation of interesting quantum phenomena such as quantum tunneling of the Néel vector,[10] S-mixing effect[11] and level repulsion.[12] The small number of interacting magnetic ions in MNMs allows exact calculations which can be compared directly to the experimental results.

Previously, the spin dynamics[13] and the thermodynamic properties[14] in the proximity of the LCs were studied in the homometallic Cr-based AF ring $[Cr_8F_8(O_2CC(CH_3)_3)_{16}]$-$0.25C_6H_{14}$ (abbreviated as Cr_8) with a S = 0 ground state due to AF interaction ($J_{Cr-Cr} \sim 16.9$ K) between nearest-neighbor Cr^{3+} (s = 3/2) ions. Starting from a homometallic ring structure and by substituting and/or inserting different

metallic ions in place of the transition metal magnetic ions, one can manipulate the topology of the interactions[15,16] which determines the magnetic properties and consequently LCs. One particular situation of interest in the present work is when the homometallic ring is interrupted by the presence of a diamagnetic metal ion, as in the case of Cr_8Cd,[17] recently investigated by polarized neutron diffraction.[18] Another example is $[Cr_8ZnF_9(O_2CC(CH_3)_3)_{18}](Me_2CH)_2NH_2$ (abbreviated as Cr_8Zn), where Zn^{2+} is the diamagnetic ion. Due to the presence of Zn^{2+}, the Cr_8Zn molecule can be considered a finite spin segment, thus a model system to study finite size effects.[18–20] The structure of Cr_8Zn is referred to as an "open ring," composed by eight Cr^{3+} (s = 3/2) ions and one Zn^{2+} diamagnetic ion, with S = 0 ground state. A previous study on this compound was done by means of Inelastic Neutron Scattering (INS) measurements performed on a randomly oriented microcrystalline sample.[21]

The aim of the present work is the investigation, by thermodynamic measurements and nuclear magnetic resonance (NMR) relaxation and spectroscopy, of the multiple LCs between ground and excited states in a single crystal of the Cr_8Zn finite spin segment, with an even number of magnetic ions. Single-crystal measurements allow us the direct access to the anisotropic properties of the molecule and the evaluation of the presence of anti-crossings between different spin multiplets, induced by anisotropic terms in the Hamiltonian. As remarkable results of such investigation, we find that at the LCs the *J strain* determines the broadening and shape of the magnetization and torque curves and of the nuclear spin-lattice relaxation rate (NSLR) peaks, while the Dzyaloshinskii-Moriya (DM) interaction is responsible for the energy levels repulsion.

The layout of this article is the following. In Sec. II, we first say few words about the structure of the sample and then we introduce the microscopic spin Hamiltonian used to interpret the experimental data. In Sec. III, we report the results of magnetization, specific heat, and torque measurements, as a function of the magnetic field for several temperatures below 2 K, which are well reproduced by using the spin-Hamiltonian introduced in Section II. In Sec. IV, we make use of proton Nuclear Magnetic Resonance (NMR) to measure the nuclear spin-lattice relaxation rates ($1/T_1$) and the NMR signal loss (wipe-out effect) as a function of the magnetic field. These two effects are analyzed at the level crossing in terms of quasi-elastic and inelastic contributions to the nuclear relaxation. The summary and conclusions are presented in Sec. V.

II. THEORY

The synthesis, structure, and characterization of the here used single crystals of Cr_8Zn are described in Ref. 22; for Cr_8 see Ref. 13 and references therein. In Fig. 1 a drawing of the Cr_8Zn and Cr_8 structure, where the typical ring-like arrangement of the Cr^{3+} (s = 3/2) and/or Zn^{2+} (s = 0) metal ions, is reported.

The microscopic description of the heteronuclear open-ring Cr_8Zn is based on the following spin Hamiltonian:

$$H_0 = J_{Cr-Cr}\sum_{i=1}^{7}\mathbf{S}_i\cdot\mathbf{S}_{i+1} + d\sum_{i=1}^{8}S_{zi}^2 + e\sum_{i=1}^{8}(S_{xi}^2 - S_{yi}^2) + \sum_{i>j=1}^{8}\mathbf{S}_i\cdot\mathbf{D}_{ij}\cdot\mathbf{S}_j + g\mu_B\mathbf{H}\cdot\sum_{i=1}^{8}\mathbf{S}_i, \quad (1)$$

where $\mathbf{S}_i$ is the spin operator of the i-th Cr ion in the ring. In the following, we assume that the site $i = 9$ is occupied by the Zn^{2+} ion. The first term in Eq. (1) describes the isotropic Heisenberg exchange interaction between pairs of nearest neighboring Cr^{3+} ions, with strength J_{Cr-Cr}. The second and third terms account for single ion zero-field splitting anisotropy (with the z axis perpendicular to the plane of the ring) and the next one is the magnetic dipole-dipole interaction. The elements of the coupling tensor $\mathbf{D}_{ij}$ are calculated in the point-dipole approximation. The last term represents the Zeeman interaction with an external magnetic field $\mu_0\mathbf{H}$, with isotropic and uniform g for all Cr^{3+} ions.

The minimal model introduced in Eq. (1), with uniform exchange couplings and zero-field splitting tensors along the whole ring, is sufficient to provide a good description of low-temperature magnetization and specific data, which are shown in Sec. III. They are well reproduced by assuming $J_{Cr-Cr} = 1.32\ (4)$ meV, $d = -28(5)\mu$ eV and $|e| = 3(3)\ \mu$ eV

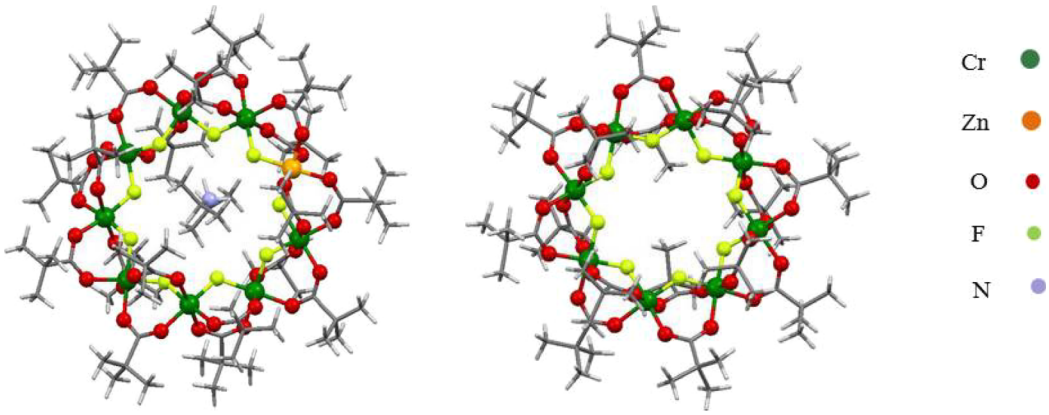

FIG. 1. Structure of Cr_8Zn (a) and Cr_8 (b). Hydrogen atoms are omitted for clarity.

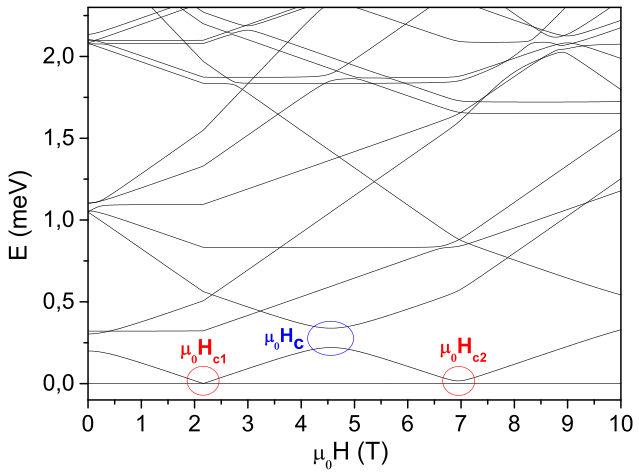

FIG. 2. Magnetic field dependence of the low-lying energy levels of Cr_8Zn calculated according to Eq. (2), with $J_{Cr-Cr} = 1.32$ meV, $d = -28\mu$ eV, and $|e| = 3\mu$ eV. The field lies in the plane of the ring. The two ground state level crossings fields $\mu_0 H_{c1}$ and $\mu_0 H_{c2}$ are indicated in red, while the excited states level anti-crossing $\mu_0 H_c$ is indicated in blue. The energy of the ground state is set to zero for each value of the magnetic field.

(note that the here-reported errors are based on a combined analysis of previous INS data[21] and current thermodynamic and NMR measurements) in agreement with the model used to fit INS data in Ref. 21. The theoretical curves are obtained by numerically diagonalizing the Hamiltonian as described in Ref. 12. With the calculated eigenstates and eigenvalues, the field dependence of the magnetization M, and of the specific heat as well as torque measurements can be evaluated and compared with the experimental results (see Sec. III).

An external magnetic field lifts the degeneracy of the M_s levels inducing level crossings between the ground and excited states (Fig. 2). According to the results of the diagonalization of Eq. (1) the first two ground state level crossings are expected at $\mu_0 H_{c1} = 2.15$ T and $\mu_0 H_{c2} = 6.95$ T (red circles in Fig. 2), where $|S = 0, M_s = 0\rangle$ crosses $|S = 1, M_s = -1\rangle$ and $|S = 1, M_s = -1\rangle$ crosses $|S = 2, M_s = -2\rangle$, respectively. As shown below, torque measurements at different angles suggest the presence of a sizeable level-repulsion at 6.95 T, which is not predicted by Hamiltonian (1). This is also in agreement with NMR nuclear spin-lattice relaxation rate experimental results and can be modeled by adding a DM interaction term perpendicular to the plane of the ring, i.e., by assuming

$$H = H_0 + H_{DM} \tag{2}$$

with

$$H_{DM} = G_Z \sum_{i=1}^{7} (S_{xi} S_{yi+1} - S_{yi} S_{xi+1}). \tag{3}$$

It is worth noting that, although other ways can be found to obtain an anti-crossing between S = 2 and S = 1 multiplets, this mechanism is able to reproduce the correct angular dependence of the torque (see discussion below). In addition, we stress that the introduction of H_{DM} with G_z determined from torque measurements does not alter the interpretation of other experimental results. Indeed, magnetization and specific heat data can be fitted also with the simplified model of Hamiltonian (1) and are only marginally affected by the introduction of H_{DM}. Anyway, the calculations reported below are all performed by considering the whole Hamiltonian (2), including DM interaction.

The field-dependence of the energy levels, calculated by using Hamiltonian (2), is shown in Fig. 2. This model yields a very small ground state anti-crossing at $\mu_0 H_{c1}$ and a sizeable one at $\mu_0 H_{c2}$. The excited states level anti-crossing H_c shown in the blue circle of Fig. 2 is also predicted and experimentally verified by specific heat and NMR measurements.

III. THERMODYNAMIC PROPERTIES

A. Experimental methods

Magnetization M(H) and specific heat C(H) measurements have been performed in house by means of a cryomagnetic system with ^{3}He insert that allows to reach temperatures as low as 0.3 K and a superconducting coil operating up to $\mu_0 H = 7$ T. All measurements have been done on Cr_8Zn single crystals. Magnetization was measured by Hall probes made of 2DEG semiconducting heterojunctions.[23] We have collected specific heat data in a commercial calorimeter, using a thermal relaxation method under quasi-adiabatic conditions. The single-crystal sample of Cr_8Zn was thermalized by Apiezon N grease, whose contribution was subtracted by means of a phenomenological expression. High field torque and heat capacity measurements have been performed at LNCMI laboratory in Grenoble (F). In this case, heat capacity measurements were carried out with a homemade calorimeter by using the AC calorimetry technique.[26] We used CuBe cantilever with capacitance read out to measure magnetic torque as described in Ref. 24. The experimental apparatus was sensitive to the y component of the torque vector (T_y) acting on the sample in a magnetic field **H**, which was applied in the xz plane at an angle θ from z, that is, the axis perpendicular to the common (Cr_8Zn) ring's plane. Rotations of the sample were performed around the y axis (see inset Fig. 6(a)).

1. Magnetization

We first present our experimental results for the magnetization versus field M (H) at low temperatures, with the magnetic field lying in the plane of the ring (θ = 90°). A clear step-like increase in magnetization is observed for temperatures up to 1 K, while at T = 2 K the magnetization is approximately proportional to the field (Fig. 3(a), full symbols). At low magnetic fields ($H < H_{c1}$), M is observed to be zero as a direct evidence of a singlet ground state, while the magnetization rapidly increases at 2.15 and 6.95 T, corresponding to the first and second ground state level (anti)crossings. The calculations of M vs H and of dM/dH are reported in Figs. 3(a) and 3(b), respectively. As stated above, even if the effect of the additional DM term (Eq. (3)) on the magnetization is found to be negligible, the theoretical (continuous) curves reported in Fig. 3 are calculated by numerically diagonalizing the full spin Hamiltonian (2).

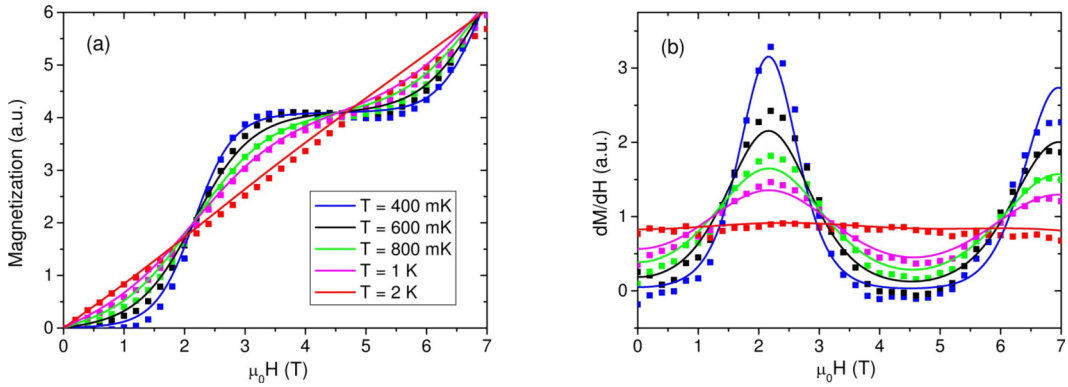

FIG. 3. Magnetic field dependence of the magnetization (a) and of dM/dH (b) measured at T = 0.4, 0.6, 0.8, 1, 2 K, with the magnetic field applied in the plane of the ring (θ = 90°). Solid lines show the theoretical calculations resulting from Eq. (2), with a Gaussian distribution of the exchange constants (*J-strain*) with standard deviation $\sigma_J = 0.04\ J$.

We note that the measured peak in dM/dH centered at H_{c2} appears to be broader than the one centered at H_{c1}. This could be due to a distribution of parameters in the spin Hamiltonian resulting from some local disorder (*J-strain*). In particular, different molecules in the crystal could have slightly different values of J. This, in turn, implies a distribution of values of the crossing fields centered at the nominal $\mu_0 H_{c1}$ or $\mu_0 H_{c2}$. Notice that the effect of *J-strain* is much more pronounced in the proximity of $\mu_0 H_{c2}$ than $\mu_0 H_{c1}$, since the exchange energy gap between the S = 2 and S = 1 multiplets (which cross at $\mu_0 H_{c2}$) is about three times the exchange energy gap between the S = 1 and S = 0 multiplets, involved in the crossing at H_{c1}. Hence, we observe a change induced by a given variation of J three times as large on H_{c2} with respect to H_{c1}, i.e., $\frac{\partial H_{c2}}{\partial J} \approx 3\frac{\partial H_{c1}}{\partial J}$. This behavior explains the much more pronounced broadening of the peak at $\mu_0 H_{c2}$ when compared to the one at $\mu_0 H_{c1}$. We have reproduced this broadening by introducing a Gaussian distribution of the exchange constant J, with standard deviation $\sigma_J = 0.04\ J$, in line with what assumed for Cr_7Ni in Ref. 25. The reported value of σ_J was also used to fit the broadening effects in the torque and in the NMR nuclear-spin-relaxation measurements as will be shown in Sec. IV.

2. Specific heat

Measurements of specific heat at low temperature as a function of the external magnetic field have been proved to be very useful to investigate level crossing effects also in the presence of a gap at the critical crossing field leading to a level anticrossing (LAC).[11,14] The magnetic contribution to the specific heat is computed, starting from the eigenvalues E_n of the spin Hamiltonian,

$$\frac{C}{R} = \beta^2 \frac{\sum_n E_n^2 e^{-\beta E_n} \sum_n e^{-\beta E_n} - \left[\sum_n E_n e^{-\beta E_n}\right]^2}{\left[\sum_n E_n e^{-\beta E_n}\right]^2}, \qquad (4)$$

where $R = 8.314$ J mol^{-1} K^{-1}, $\beta = -1/k_B T$, and $Z = \sum_n e^{-\beta E_n}$ is the partition function. Expression (4) can be useful to understand the behavior of the specific heat at low temperature and close to a LC, where the investigated system can be approximated as a two level system. In fact for a two level system Eq. (4) reduces to

$$\frac{C}{R} = \left[\frac{\Delta(H)}{k_B T}\right]^2 \frac{\exp\left[\frac{\Delta(H)}{k_B T}\right]}{\left\{1 + \exp\left[\frac{\Delta(H)}{k_B T}\right]\right\}^2}. \qquad (5)$$

Eq. (5) indicates that when the magnetic field is varied the specific heat should reach a maximum when $\Delta(H) \approx 2.5 k_B T$ (Schottky anomaly). In the presence of a level crossing one should thus observe two peaks in the specific heat plotted vs. external magnetic field with a dip in the middle centered at the crossing field, as a result of a double Schottky anomaly. In particular, in presence of a pure level crossing, the dip between the two Schottky peaks should go down to zero, while in presence of a level repulsion (LAC) the dip can be much less pronounced and it gives a direct measurement of the gap at the anti-crossing.[11,14]

The specific heat for the magnetic field applied in the plane of the ring (θ = 90°) is shown in Fig. 4 at three different temperatures (points) and compared to the simulated behavior (lines), obtained from the eigenvalues of spin Hamiltonian (2).

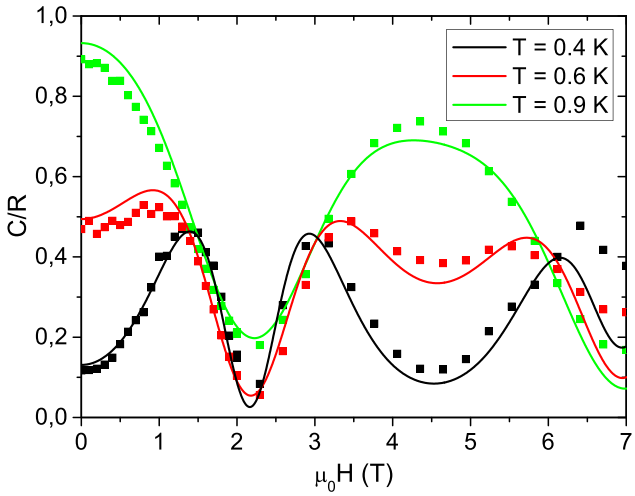

FIG. 4. Magnetic field dependence of the specific heat measured at T = 0.4, 0.6, 0.9 K, with θ = 90°. Solid lines show the theoretical calculations obtained from spin Hamiltonian (2).

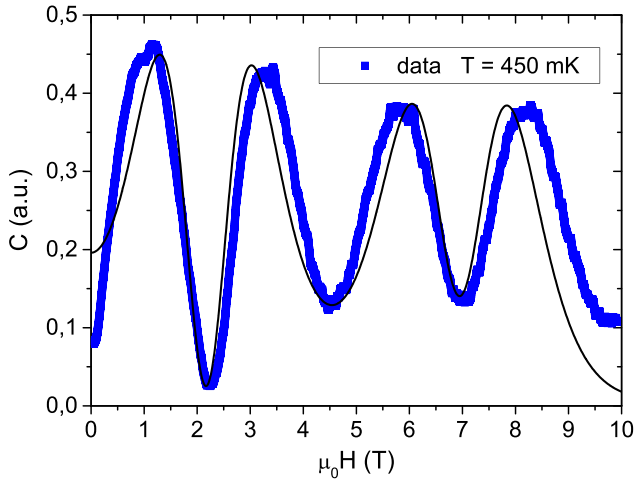

FIG. 5. Specific heat as a function of magnetic field at T = 0.45 K. The solid lines represent the specific heat calculated by Eq. (5) with the energy levels determined from the diagonalization of Hamiltonian (2) by including both the DM interaction (which induces a level repulsion at $\mu_0 H_{c2}$) and of the *J-strain* effects.

As can be seen, the theoretical curves are in good agreement with the experimental results. The small disagreement found for the peak at T = 0.4 K at high magnetic field is within the experimental accuracy considering that a small temperature drift is possible at such low T.

The uncertainty in the subtraction of the non-magnetic background contributing to the specific-heat (which is a particularly hard task) limits the precision in determining the size of possible anti-crossing in the ground state. The minimum at $\mu_0 H_{c1}$ = 2.15 T is in good agreement with the curves calculated from spin Hamiltonian (2). Moreover, the experimental evidence of level-repulsion between the excited multiplets S = 2 and S = 0 at $\mu_0 H_c$ = 4.5 T (see minimum in Fig. 4 at T = 0.4 K) is well reproduced by our model, as it can be observed in the level scheme reported in Fig. 2 (blue circle).

In order to gain deeper insight into the energy gap evolution for the second level crossing field, we have also performed specific heat measurements up to 10 T at the High Magnetic Fields Laboratory in Grenoble. We find again a good agreement between experimental data and the theoretical curves (Fig. 5) obtained from spin Hamiltonian (2). The anti-symmetric exchange interaction (Eq. (3)) (which induces a sizeable anti-crossing at $\mu_0 H_{c2}$), as well as the Gaussian broadening of the exchange constants, is responsible for the non-zero value of the specific heat at $\mu_0 H_{c2}$. The additional broadening of the fourth experimental peak can be ascribed to heating of the sample for large H, as the result of the technique here employed, i.e., AC calorimetry combined with a continuous sweeping of the applied magnetic field.

3. Torque magnetometry

In order to get independent information on the ground state level crossings, we have performed torque measurements at different angles. As shown in Fig. 6(a), the experimental magnetic torque signal at T = 50 mK (simulated as described in Ref. 24, Fig. 6(b)) presents the typical step-like behavior due to the transitions of the ground state to multiplets with progressively higher S values.[27] Torque measurements on Cr_8Zn at the higher LC field show the presence of a small peak for an angle θ = 49.9°, which is absent at the other reported angles (−2°, 9°). A peak in the torque suggests the presence of an avoided crossing.[28] As discussed in one of our previous works[29] an anti-crossing between S = 2 and S = 1 multiplets (with the correct angular dependence) can occur due to the presence of a small—but finite—Dzyaloshinskii-Moriya interaction. Other mechanisms can induce a level repulsion at $\mu_0 H_{c2}$, such as the introduction of local anisotropy axes slightly tilted from the z-axis of the magnetic field or the assumption of non-uniform d_i values. However, we have checked that the angular dependence of the anti-crossing, together with the size of the induced gap, is not easily reproduced by Hamiltonians taking into account the tilting of local anisotropy axes and/or non-uniform d_i's. Conversely, the inclusion of a DM term (Eq. (3)) in the spin Hamiltonian leads to the appearance of a peak in the simulated torque at 49.9° which is very small or absent at the other measured angles, as shown in Fig. 6(b). For simplicity, we have not included G_x and G_y component of the DM interaction, since their contribution is very small. A good fit (Fig. 6) is obtained by fixing G_z = 0.016(5) meV = 0.012 J. This is in agreement with the theoretical model,[30] which predicts $G \approx \frac{2-g}{2} J$. Since for Cr^{3+} g = 1.98 we should expect $G \approx J/100$, which is close to the fitted parameter. The

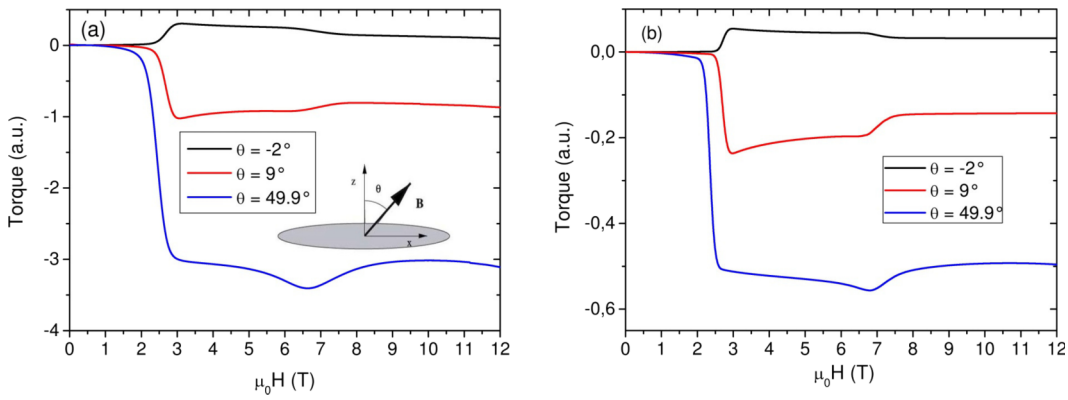

FIG. 6. Magnetic torque signal taken at the High Magnetic Fields Laboratory in Grenoble on Cr_8Zn single crystal at T = 50 mK: (a) experimental data (inset: experimental set up); (b) theoretical simulations.

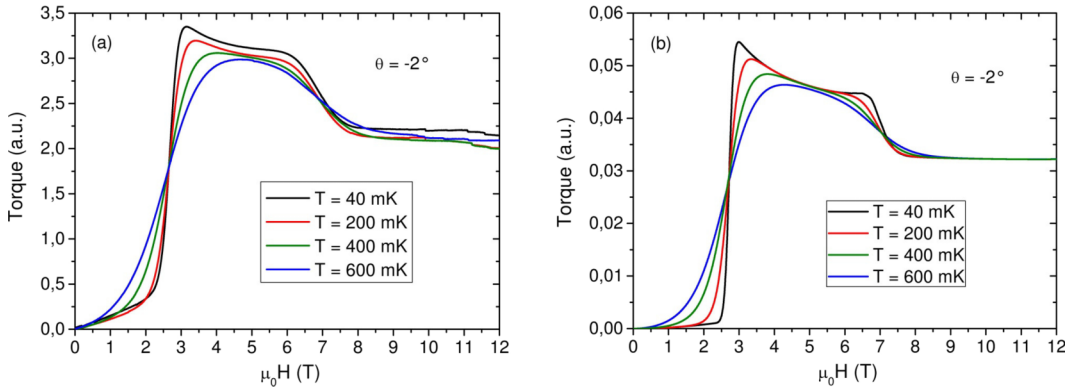

FIG. 7. Field dependence of the torque signal taken at $\theta = -2°$ on Cr_8Zn single crystal for several temperatures, reported in the legend: (a) experimental data; (b) theoretical simulations.

situation is different from the odd-numbered open-ring Cr_7Zn, in which a sizeable S-mixing and level repulsion is induced by uniform single-ion and axial anisotropies.[27] In Fig. 7, we plot the experimental data (Fig. 7(a)) of the torque at various temperatures and the results of the theoretical calculations (Fig. 7(b)).We note that the experimental peaks (Fig. 7(a)) are well reproduced by assuming the Gaussian distribution of the exchange constants discussed above, with $\sigma_J = 0.04\ J$. The introduction of *J-strain* allows us to obtain theoretical peaks with broadening in agreement with the experimental one (in contrast to the narrower peaks given by calculations when this effect is neglected).

IV. ^{1}H NMR: EXPERIMENTAL RESULTS AND ANALYSIS

A. Experimental methods

We present in this section ^{1}H NMR measurements, including nuclear spin-lattice relaxation rate, $1/T_1$, spin-spin relaxation rate, $1/T_2$, and NMR spectra in a Cr_8Zn single crystal as a function of magnetic field at low temperature (~1.7 K). Measurements were performed with the external magnetic field approximately in the ring plane, i.e., perpendicular to the molecular z-axis of the rings ($\theta = 90°$). The value of $1/T_1$ is determined by monitoring the recovery of the longitudinal nuclear magnetization measured by the spin-echo $\pi/2_x$-$\pi/2_y$ pulse sequence by means of a standard TecMag Fourier transform pulse NMR spectrometer, following a saturation comb of rf pulses. The nuclear magnetization recovery curves show magnetic field dependent multi-exponential behavior due to the presence of nonequivalent groups of ^{1}H sites in the molecule. In most cases the recovery curve can be fitted with two exponential functions leading to a fast and a slow component of the relaxation. The fast component represents a weighted average of the rates of the inequivalent protons in the molecule which are close to the magnetic ions and are thus sensing the spin dynamics. Transverse relaxation measurements, $1/T_2$, were performed by using a standard $\pi/2_x$-$\pi/2_y$ pulse sequence. ^{1}H NMR spectra were collected by using the magnetic field sweep technique[31] at three different fixed Larmor frequencies corresponding to magnetic fields smaller (51.1 MHz) and larger (234.16 MHz) than the first ground state level crossing, and at a field (340.6 MHz) larger than the second ground state level crossing.

1. Spin-lattice relaxation rate

We are now going to present and analyze the results of proton nuclear spin-lattice relaxation rate near the level crossings at low temperature in Cr_8Zn. Our aim is to gain insights on the spin dynamics at level crossing. The theory of NSLR in molecular magnets at low temperature can be derived from the basic theory of NSLR in magnetic systems developed by Moriya both for paramagnets and for antiferromagnets.[32] At high temperatures (k_BT >> J), a molecular magnet behaves as a simple paramagnet and one can apply the standard theory of nuclear relaxation in a paramagnet. However, at low temperature Moriya's theory of nuclear relaxation in antiferromagnets cannot be applied without some modifications. The problem arises from the fact that in molecular magnets the energy levels are discrete and well separated in energy as shown in Fig. 2. Thus, since there is not a continuum of spin-wave excitations, like, e.g., in a 3D antiferromagnet, no energy conserving direct relaxation transitions between the nuclear Zeeman levels and magnetic spin excitations are possible except at the level crossing. Semi-phenomenological models have been developed to describe NSLR near level crossing[33,34] and the expressions obtained have been utilized to explain the experimental results in molecular magnets.[35] We will adopt here the expression for the NSLR which was utilized to analyze the level crossing results in several AF ring-like, e.g., Cr_8,[13]

$$\frac{1}{T_1} = \chi T A^2 \left[\frac{\Gamma_1(T)}{\Gamma_1^2(T) + \omega_L^2} + \frac{\Gamma_2(T)}{\Gamma_2^2(T) + (\omega_L - \Delta_i)^2} \right]. \quad (6)$$

Here, we limit the discussion to a qualitative explanation of the two contributions appearing in Eq. (6). The first contribution is the quasi-elastic term which arises from the fluctuations of the magnetization of the molecule in the first magnetic excited state. These fluctuations due to spin phonon interaction are modeled with a Lorenzian broadening of width Γ_1 of the magnetic state whereby the NSLR is simply proportional to the Lorenzian spectral density function at the Larmor frequency ω_L. The second term is the inelastic term which arises from direct transitions between nuclear Zeeman states accompanied

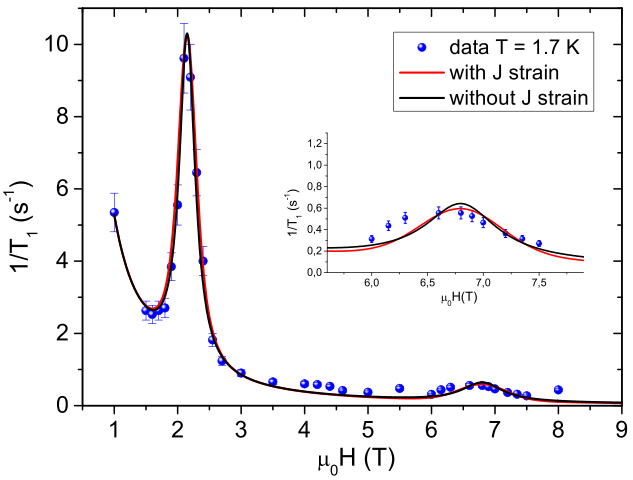

FIG. 8. ^{1}H spin-lattice relaxation as a function of magnetic field in Cr_8Zn at T = 1.7 K. The solid line is the fit according to Equation (6), including (red) or neglecting (black) *J strain* effects. The red fit is able to better reproduce the line-shape, by assuming smaller gaps, in agreement with model Hamiltonian (2) and with thermodynamic measurements. The inset is a zoom close to the second level crossing.

by a transition in the magnetic state of the molecule, with broadening Γ_2. This term is important only when the applied magnetic field is very close to a level crossing value and becomes dominant when the gap Δ_i is of the order of the broadening Γ_2. The constant A^2 in Eq. (6) is the average square of the dipolar interaction between protons and magnetic ions and is temperature and field independent. In the case of Cr_8Zn the term χT in Eq. (6) is also a constant since we are considering the NMR measurements at fixed temperature (1.7 K) and the susceptibility χ = dM/dH is almost field independent as the result of thermal broadening, as shown in Fig. 3 of Sec. III A. This situation is clearly distinguished from the one found in Cr_8 where the field dependence of χT leads to a peak at LC with both elastic and inelastic contributions, which are thus difficult to separate.[13]

The NSLR experimental results as a function of the external magnetic field are shown in Fig. 8. The peak at the level crossings could be fitted by Eq. (6) with the gap between the ground and the first excited state expressed as

$$\Delta_i = \sqrt{\delta_{i-1,i}^2 + [g\mu_B\mu_0(H_{Ci} - H)]^2}, \qquad (7)$$

where $i = 1, 2$ for the first (μ_0H_{c1}) and the second (μ_0H_{c2}) level crossing, respectively. $\delta_{i-1,i}$ represents the level repulsion gap leading to a level anti-crossing.

If *J strain* effects are completely neglected, the experimental data can be fitted but large values of the anti-crossing gaps (black line in Figure 8) must be assumed: δ_{01} = 0.09 K and δ_{12} = 0.56 K which are not in agreement with the thermodynamic results and the theoretical predictions. Thus, we decided to include in the fitting the effect of *J strain* due to a distribution of *J* values as described in Section III A. We performed a fit (red line in Fig. 8) based on Eq. (6), by assuming a distribution of the crossing fields, H_{c1} and H_{c2}, induced by the Gaussian distribution of the exchange constants discussed above (Sec. III A), with standard deviation $\sigma_J = 0.04$ *J*. The values of the anti-crossing gap obtained from the fit are now in agreement with those predicted by the model (Eq. (2)) used to explain torque measurements: δ_{01} = 0.01 K at μ_0H_{c1} and δ_{12} = 0.19 K at μ_0H_{c2}. Furthermore, the inclusion of *J strain* explains the significantly more pronounced broadening of the peak at μ_0H_{c2} when compared to the one at μ_0H_{c1} (see full points in Fig. 8). The magnetic field for LC which fits the first peak in Fig. 8 is H_{c1} = 2.15 T, in good agreement with the values derived from magnetization and specific heat, while the second peak is centered at 6.8 T. This value is slightly lower than the one inferred from thermodynamic measurements (6.95 T) but still compatible within the error bar of 0.1 T.

The other parameters obtained from the fit of the first peak in Fig. 8 are: $A^2 = 5.7 \times 10^{11}$ (rad^2 mol)/(s^2 emu K) = 0.14×10^{12} rad^2/s^2, $\Gamma_1 = 1.4(0.14) \times 10^6$ rad/s, $\Gamma_2 = 2.4(0.14) \times 10^{10}$ rad/s while the χT(= 0.46 emu K/mol) comes from the magnetization measurements. The parameters used in the fit of the second LC in the inset of Fig. 8 are $A^2 = 5.7 \times 10^{11}$(rad^2 mol)/(s^2 emu K) = 0.14×10^{12} rad^2/s^2,$\Gamma_1 = 1.5(0.15) \times 10^6$ rad/s, $\Gamma_2 = 0.2 \times 10^{10}$ rad/s.

It is interesting to note that the order of magnitude of Γ_1, as determined above for the quasielastic contribution, is close to one obtained from extrapolating at low temperature the temperature dependence of the correlation frequency derived from the analysis of the NSLR results in Cr_8[35] and Cr_8Zn[36] at higher temperature. This comparison indicates that far from level crossing the NSLR is determined at all temperatures by the phonon-induced relaxation dynamics. Also the value of A^2 is in reasonable agreement with the one obtained in Cr_8.[13] The values of the interaction parameter A^2 and of the broadening parameter Γ_1 are the same at both the first and the second LC.

2. NMR line broadening

The inhomogeneous broadening occurring at high magnetic field when the molecular ring is in a magnetic ground state is shown in the representative spectra displayed in Fig. 9.

As it shown in Fig. 9, for fields lower than the first LC ($\mu_0H < 2.2$ T), the system is in the S = 0 ground

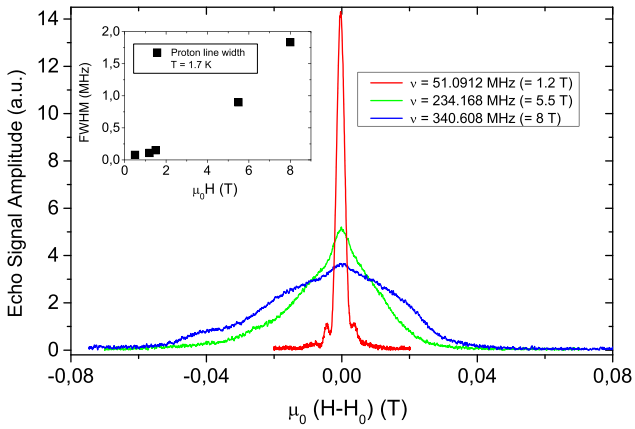

FIG. 9. Low temperature ^{1}H NMR spectra at three different resonance frequencies, i.e., different magnetic fields. Inset: the proton line width as a function of magnetic field at T = 1.7 K.

state where the local magnetic moment is also zero due to quantum fluctuation of spins. Thus, below the first LC a narrow ^{1}H NMR spectrum is observed at the frequency 51.0912 MHz ($\mu_0 H = 1.2$ T). The width is due to the nuclear-nuclear dipolar interaction plus an inhomogeneous contribution due to the distribution of local fields generated at the non-equivalent protons sites by the small average moment of the Cr spins due to the thermal molecular population of the first magnetic excited state. The second spectrum (green one) was measured at 234.168 MHz where the system becomes magnetic as the result of the first level crossing. In the magnetic state the average moment of the Cr ions is larger and consequently the inhomogeneous broadening becomes also larger and dominant. For fields above the second level crossing, the ground state becomes even more magnetic and correspondently the broadening increases. Over the whole field range the proton NMR line width is approximately proportional to the external magnetic field as shown in the inset of Fig. 9, indicating that the molecular ring remains in a paramagnetic state without spin freezing.

V. SUMMARY AND CONCLUSIONS

To conclude, the comparison of single-crystal Cr_8Zn AF ring NMR investigation with torque and specific heat measurements confirms the presence of an almost zero level repulsion gap at the first ground state LC and a small (but finite) anti-crossing gap at the second LC. This proves that combined techniques like torque magnetometry, NMR, and specific heat as well as magnetization measurements provide a powerful tool to study the level crossing mechanisms in molecular clusters. The experimental data are interpreted by introducing a minimal spin model Hamiltonian, in which the presence of level repulsion at the second LC is accounted for by the inclusion of a Dzyaloshinskii-Moriya interaction. The first two ground state level crossings were found at $\mu_0 H_{c1} = 2.15$ T and $\mu_0 H_{c2} = 6.95$ T. While magnetization measurements are not able to distinguish between a true level crossing or a small anti-crossing, torque measurements at different angles, together with NSLR measurements, indicate the presence of a small, but finite, energy gap at the second level LC. The broadening of the peaks in torque, magnetization and $1/T_1$ suggests a distribution of parameters in the spin Hamiltonian due to local disorder (*J strain*), compatible to a similar effect observed in Cr_7Ni. The *J strain* has thus been demonstrated to have, together with Dzyaloshinskii-Moriya interaction, a crucial role in the behavior of such quantities at energy level crossings in finite spin segments.

Remarkably, the NMR spin-lattice relaxation rate shows a peak at LC's which has been shown to be due entirely to inelastic nuclear relaxation mechanism in contrast with Cr_8, where both elastic and inelastic contributions are present at LC.[13] The enhancement of the NSLR at LC is also responsible for a loss of the NMR signal. This wipe-out effect which was observed for the first time at level crossing in molecular magnets and it is explained in terms of the enhancement of the spin-spin relaxation rate $1/T_2$ around the critical crossing field in agreement with the enhancement of $1/T_1$, both being due to the strong inelastic nuclear spin-lattice relaxation at the almost gapless level crossing.

ACKNOWLEDGMENTS

This work was financially supported by the Italian FIRB Project No. RBFR12RPD1 of the Italian MIUR "New Challenges in Molecular Nanomagnetism: From Spin Dynamics to Quantum-Information Processing." Very useful discussions with P. Santini, G. Amoretti, G. Allodi, and R. De Renzi are gratefully acknowledged. L. Bordonali and M. Mariani are acknowledged for help in some experimental measurements.

APPENDIX: THE WIPE-OUT EFFECT

An interesting effect (wipe-out) is observed at the level crossing consisting in a loss of NMR measured signal intensity around the critical fields. While such wipe-out effect was previously observed in molecular magnets by studying the NMR signal as a function of the temperature, in the present work, we report the first observation of a wipe-out effect as a function of external magnetic field. The effect is shown in Fig. 10 where we report the amplitude of the measured proton NMR signal $M_{xy}(0)$ divided by the applied magnetic field in order to eliminate the effect of the Boltzmann population of the nuclear Zeeman levels, as a function of H. The absolute value of the proton NMR signal was determined by the echo amplitude of the decay curve extrapolated back at $t = 0$, considering that the decay of the echo signal follows an exponential law over the whole delay time range.

We analyze the effect by means of the model introduced in Ref. 37. The starting point is the description of the mechanism for the irreversible decay of the nuclear magnetization which is described by the spin-spin relaxation rate parameter $1/T_2$. In a nonmagnetic molecular crystal where the protons are rigid in the lattice, the transverse relaxation is due to the dipolar interaction among the proton nuclei. This dipolar contribution

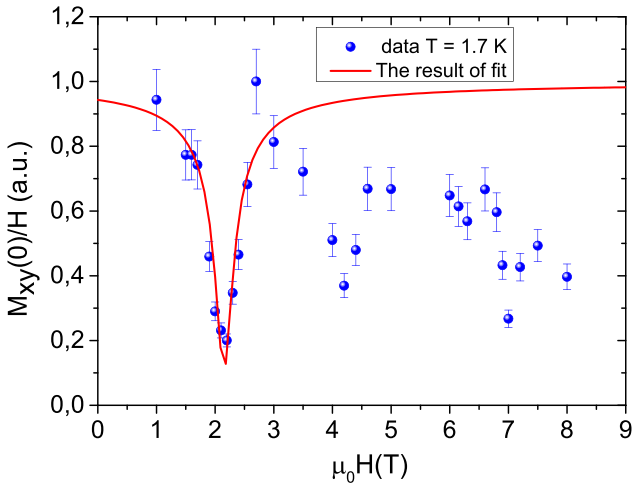

FIG. 10. The magnetic field dependence of the normalized ^{1}H NMR signal intensity, i.e., $M_{xy}(0)/H$. Solid line is the theoretical curve discussed in the text.

is T and H independent and is of the order of the inverse line-width of the NMR line, i.e., about 20 kHz. It should be noticed that this value of the NMR line-width can be observed just at high temperature (T > 150 K), as when the temperature is decreased the nuclei are subjected also to the hyperfine interaction with the magnetic ions, which broadens sensibly the spectrum. This interaction has a static component which determines an inhomogeneous broadening of the NMR line which generates a reversible decay of the transverse nuclear magnetization which does not contribute to T_2. On the other hand, the time dependence of the hyperfine interaction generates spin-lattice and spin-spin nuclear relaxation. Based on weak collision theory and fast motion approximation, $1/T_2$ can be expressed in terms of the spectral density of the fluctuating hyperfine field at zero frequency as[38,39]

$$\frac{1}{T_2} \approx \frac{1}{T_2}\Big]_{f(\omega=0)} = \gamma_N^2 \left\langle \delta H_Z^2 \right\rangle f(\omega = 0) = \gamma_N^2 \frac{\left\langle \delta \mu_e^2 \right\rangle}{r^6} f(\omega = 0), \tag{A1}$$

where$\gamma_N^2 \left\langle \delta H_Z^2 \right\rangle$ is the average square of the nuclear-electron dipolar interaction whereby δH_Z is the local longitudinal fluctuating field originating from a magnetic moment sitting at a distance r apart from the proton spin. The spectral density function, $f(\omega)$, is the Fourier Transform of the correlation function

$$f(\omega) \propto \int \left\langle S_{j+}(t) S_{j-}(0) \right\rangle e^{-i\omega t} dt. \tag{A2}$$

By assuming for the time dependence of the two-spin correlation function in Eq. (A2) an exponential function with a time constant τ (correlation time), from Eqs. (A1) and (A2) one has

$$\frac{1}{T_2} = \gamma_N^2 \frac{\left\langle \delta \mu_e^2 \right\rangle}{r^6} \tau(H,T). \tag{A3}$$

The correlation time can be temperature or magnetic field dependent and the validity of Eq. (A3) ceases when one crosses the limit of the fast motion approximation, namely, when τ becomes of the order of the inverse of the interaction frequency $\omega = \gamma_n \delta$ H_z with γ_n the nuclear gyromagnetic factor. In the slow motion approximation, the nuclear-electron hyperfine interaction becomes static and it generates an inhomogeneous broadening of the NMR line. Normally the contribution to $1/T_2$ described by Eq. (A3) is negligible compared to the nuclear dipolar interaction and can be disregarded. However, in presence of slowing down of the magnetic fluctuations or, as in our case, in the vicinity of a LC this contribution can become dominant and be responsible for the wipe-out effect. In fact the dependence of $1/T_2$ from the distance r of the inequivalent protons with respect to the magnetic ions gives rise to distribution of $1/T_2$ values. As a result, when the correlation time of the magnetic ions becomes gradually longer T_2 becomes shorter and eventually crosses the limiting value of the instrument τ_d, below which the signal cannot be detected in the experimental setup. In addition, if this increase of the correlation time is assumed to be monotonic, it is expected that the critical value of τ is progressively reached by all the proton sites, with the ones closer to magnetic ions being wiped out first, generating a gradual loss of the NMR signal intensity.

In order to obtain a quantitative model one can assume one central magnetic ion surrounded by a large number of protons uniformly distributed at distance up to a maximum value R^*, the number density being $\rho = n_0/[(4\pi/3)R^*]$ where n_0 is the total number of protons in each molecule. Being in the regime of the wipe-out effect, and for a certain value of the correlation time, there is a certain number of protons having a T_2 value faster than the critical value. These protons are enclosed within a notional sphere of radius r_c and do not contribute to the measured signal intensity. On the other hand, the protons located outside this sphere can be detected and their number $n(T,H)$ can be written as

$$n(T,H) = n_0[1 - \left(\frac{r_c}{R^*}\right)^3]. \tag{A4}$$

The value of the critical radius r_c in Eq. (A4) can be obtained from Eq. (A3) setting $T_2^{-1} = \tau_d^{-1}$. Then one can express $n(T,H)$ in terms of τ as[37]

$$\frac{n(T,H)}{n_0} = 1 - \frac{\gamma_N \sqrt{\tau_d} \sqrt{\left\langle \delta \mu_e^2 \right\rangle}}{R^{*3}} \sqrt{\tau(T,H)}. \tag{A5}$$

Eq. (A5) describes the wipe-out effect due to the slowing down of the fluctuations upon lowering the temperature.

In the present work, we extend this model for the wipe-out effect at the level crossing. Thus, we redefine the meaning of the correlation time τ in Eq. (A5). This can be done by observing that the inelastic term in Eq. (6) contains the spectral density of the fluctuations at the Larmor frequency. Since according to Eq. (A1), the spin-spin relaxation rate depends on the spectral density of the fluctuations at zero frequency one has

$$\frac{1}{T_2} \propto f(0) \propto \lim_{\omega_L \to 0} \left(\frac{\Gamma_2(T)}{\Gamma_2^2(T) + (\omega_L - \Delta_1)^2} \right) \approx \frac{\Gamma_2(T)}{\Gamma_2^2(T) + \Delta_1^2} \approx \tau^*(H). \tag{A6}$$

We have made the tacit assumptions that the spectral density of the transverse hyperfine field fluctuations entering the $1/T_1$ theory is the same as the spectral density of the longitudinal (with respect to the external magnetic field) fluctuations entering the $1/T_2$ theory. The assumption should be valid for an isotropic Heisenberg magnetic system.

By replacing in Eq. (A6) the effective correlation time τ^* (H) defined in Eq. (A5) one finally obtains

$$\left(\frac{M_{xy}(0)}{H}\right) \propto \frac{n(T,H)}{n_0} = 1 - A\sqrt{\frac{\Gamma_2(T)}{\Gamma_2^2(T) + \Delta_1^2}}, \tag{A7}$$

where A, a constant parameter, includes the critical value for the detection time of the instrument and the size of the limiting hyperfine interaction and Δ_1 is ascribed to the gap between the ground state and the first excited state which is given by Eq. (7). The experimental results are fitted well by Eq. (A7) (see Fig. 10) in the case of the first level crossing with parameters in agreement to those obtained from the $1/T_1$ analysis. Although this model is very approximate, it appears

to be able to interpret the wipe-out effect at LC and to confirm the importance of the inelastic mechanism for NSLR.

The other two dips in the $M_{xy}(0)/H$ graph around $\mu_0 H_c = 4.4$ T and $\mu_0 H_{c2} = 6.9$ T correspond to the first excited states LC and the second ground state LC, respectively. NMR results give evidence of the LAC at $\mu_0 H_c = 4.4$ T, in agreement (within the error-bar of 0.1 T) with specific heat measurements. Unfortunately, the analysis of the wipe-out results in Fig. 10 for these LC's is more complicate due to the combination of T_2 shortening and broadening effects of the NMR line and will not be attempted here.

[1]Z. Fu, *Spin Correlation and Excitation in Spin-frustrated Molecular and Molecule- based Magnets* (Forschungszentrum Jülich GmbH, 2011).
[2]J. W. Sharples, D. Collison, E. J. L. Mclnnes, J. Schnack, E. Palacios, and M. Evangelisti, Nat. Commun. **5**, 5321 (2014).
[3]L. Thomas, F. Lionti, R. Ballou, D. Gatteschi, R. Sessoli, and B. Barbara, Nature **383**, 145 (1996); See also, J. A. A. J. Perenboom, J. S. Brooks, S. O. Hill, T. Hathaway, and N. S. Dalal, Physica B **246-247**, 294 (1998).
[4]S. A. Owerre and J. Nsofini, e-print arXiv:1502.05684v7 (2015).
[5]*Magnetism: Molecules to Materials III*, edited by S. J. Miller and M. Drillon (Wiley-VCH, New York, 2002).
[6]F. Troiani, A. Ghirri, M. Affronte, S. Carretta, P. Santini, G. Amoretti, S. Piligkos, G. Timco, and R. E. P. Winpenny, Phys. Rev. Lett. **94**, 207208 (2005); P. Santini, S. Carretta, F. Troiani, and G. Amoretti, *ibid.* **107**, 230502 (2011); G. Aromì, D. Aguilà, P. Gamez, F. Luis, and O. Roubeau, Chem. Soc. Rev. **41**, 537 (2012); A. Chiesa, G. F. S. Whitehead, S. Carretta, L. Carthy, G. A. Timco, S. J. Teat, G. Amoretti, E. Pavarini, R. E. P. Winpenny, and P. Santini, Sci. Rep. **4**, 7423 (2014).
[7]S. Yamamoto, J. Korean Phys. Soc. **63**, 2 (2013).
[8]T. Lancaster, J. S. Möller, S. J. Blundell, F. L. Pratt, P. J. Baker, T. Guidi, G. A. Timco, and R. E. P. Winpenny, J. Phys.: Condens. Matter **23**, 242201 (2011).
[9]D. Vaknin, V. O. Garlea, F. Demmel, E. Mamontov, H. Nojiri, C. Martin, I. Chiorescu, Y. Qiu, P. Kögerler, J. Fielden, L. Engelhardt, C. Rainey, and M. Luban, J. Phys.: Condens. Matter **22**, 466001 (2010).
[10]F. Meier and D. Loss, Phys. Rev. Lett. **86**, 5373 (2001).
[11]M. Affronte, A. Cornia, A. Lascialfari, F. Borsa, D. Gatteschi, J. Hinderer, M. Horvatic, A. G. M. Jansen, and M.-H. Julien, Phys. Rev. Lett. **88**, 167201 (2002).
[12]S. Carretta, J. van Slageren, T. Guidi, E. Liviotti, C. Mondelli, D. Rovai, A. Cornia, A. L. Dearden, F. Carsughi, M. Affronte, C. D. Frost, R. E. P. Winpenny, D. Gatteschi, G. Amoretti, and R. Caciuffo, Phys. Rev. B **67**, 094405 (2003).
[13]E. Micotti, A. Lascialfari, F. Borsa, M. H. Julien, C. Berthier, M. Horvatić, J. van Slageren, and D. Gatteschi, Phys. Rev. B **72**, 020405(R) (2005).
[14]M. Affronte, T. Guidi, R. Caciuffo, S. Carretta, G. Amoretti, J. Hinderer, I. Sheikin, A. G. M. Jansen, A. A. Smith, R. E. P. Winpenny, J. van Slageren, and D. Gatteschi, Phys. Rev. B. **68**, 104403 (2003).
[15]O. Cador, D. Gatteschi, R. Sessoli, A.-L. Barra, G. A. Timco, and R. E. P. Winpenny, J. Magn. Magn. Mater. **290-291**, 55 (2005).
[16]E. J. L. Mcinnes, S. Piligkos, G. A. Timco, and R. E. P. Winpenny, Coord. Chem. Rev. **249**, 2577 (2005).
[17]A. Ghirri, A. Candini, M. Evangelisti, M. Affronte, S. Carretta, P. Santini, G. Amoretti, R. S. G. Davies, G. Timco, and R. E. P. Winpenny, Phys. Rev. B **76**, 214405 (2007).
[18]T. Guidi, B. Gillon, S. A. Mason, E. Garlatti, S. Carretta, P. Santini, A. Stunault, G. Caciuffo, J. van Slageren, B. Klemke, A. Cousson, G. A. Timco, and R. E. P. Winpenny, Nat. Commun. **6**, 7061 (2015).
[19]Y. Furukawa, K. Kiuchi, K. Kumagai, Y. Ajiro, Y. Narumi, M. Iwaki, K. Kindo, A. Bianchi, S. Carretta, G. A. Timco, and R. E. P. Winpenny, Phys. Rev. B **78**, 092402 (2008).
[20]F. Adelnia, M. Mariani, L. Ammannato, A. Caneschi, D. Rovai, R. Winpenny, G. Timco, M. Corti, A. Lascialfari, and F. Borsa, J. Appl. Phys. **117**, 17B308 (2015).
[21]A. Bianchi, S. Carretta, P. Santini, G. Amoretti, T. Guidi, Y. Qiu, J. R. D. Copley, G. Timco, C. Muryn, and R. E. P. Winpenny, Phys. Rev. B **79**, 144422 (2009).
[22]A. Ghirri, A. Chiesa, S. Carretta, F. Troiani, J. Van Tol, S. Hill, I. Vitorica-Yrezabal, G. Timco, R. Winpenny, and M. Affronte, "Coherent spin dynamics in molecular Cr_8Zn wheels," J. Phys. Chem. Lett. **6**, 5062 (2015).
[23]http://www.qdusa.com/techsupport/index.html, see MPMS, Service Notes.
[24]A. Cornia, A. G. M. Jansen, and M. Affronte, Phys. Rev. B **60**, 12177 (1999).
[25]S. Carretta, P. Santini, G. Amoretti, T. Guidi, J. R. D. Copley, Y. Qiu, R. Caciuffo, G. Timco, and R. E. P. Winpenny, Phys. Rev. Lett. **98**, 167401 (2007).
[26]P. F. Sullivan and G. Seidel, Phys. Rev. **173**, 679 (1968).
[27]S. Carretta, P. Santini, G. Amoretti, M. Affronte, A. Ghirri, I. Sheikin, S. Piligkos, G. Timco, and R. E. P. Winpenny, Phys. Rev. B **72**, 060403(R) (2005); see also G. Kamieniarz, P. Kozłowski, M. Antkowiak, P. Sobczak, T. Ślusarski, and B. Brzostowski, Acta Phys. Pol., A **121**, 992–998 (2012).
[28]O. Waldmann, S. Carretta, P. Santini, R. Koch, A. G. M. Jansen, G. Amoretti, R. Caciuffo, L. Zhao, and L. K. Thompson, Phys. Rev. Lett. **92**, 096403 (2004).
[29]F. Cinti, M. Affronte, and A. G. M. Jansen, Eur. Phys. J. B **30**, 461 (2002).
[30]T. Moriya, Phys. Rev. **120**, 91 (1960).
[31]L. Bordonali, E. Garlatti, C. M. Casadei, Y. Furukawa, A. Lascialfari, S. Carretta, F. Troiani, G. Timco, R. E. P. Winpenny, and F. Borsa, J. Chem. Phys. **140**, 144306 (2014).
[32]T. Moriya, Prog. Theor. Phys. **16**, 23 (1956); **28**, 371 (1962).
[33]A. Cornia, A. Fort, M. G. Pini, and A. Rettori, Europhys. Lett. **50**, 88 (2000).
[34]M. Luban, F. Borsa, S. Bud'ko, P. Canfield, S. Jun, J. K. Jung, P. Kögerler, D. Mentrup, A. Müller, R. Modler, D. Procissi, B. J. Suh, and M. Torikachvili, Phys. Rev. B **66**, 054407 (2002).
[35]F. Borsa, Y. Furukawa, and A. Lascialfari, *New Developments in Magnetic Resonance* (Springer and Verlag, 2006).
[36]F. Adelnia, L. Bordonali, M. Mariani, S. Bordignon, G. Timco, R. Winpenny, F. Borsa, and A. Lascialfari, J. Phys.: Condens. Matter **27**, 506001 (2015).
[37]M. Belesi, A. Lascialfari, D. Procissi, Z. H. Jang, and F. Borsa, Phys. Rev. B **72**, 014440 (2005).
[38]A. Abragam, *The Principles of Nuclear Magnetism* (Clarendon, Oxford, 1961).
[39]C. P. Slichter, *Principle of Magnetic Resonance* (Springer-Verlag, Berlin, 1989).